Research Square

Preprints are preliminary reports that have not undergone peer review.
They should not be considered conclusive, used to inform clinical practice,
or referenced by the media as validated information.

Design and Fabrication of Transtibial Prosthetic Sockets Using Fused Deposition Modeling with Tough PLA Filament: A Technical Note

Muhammad Nouman
muhammad.nou@mahidol.ac.th
Mahidol University
Teeradon Nanthasilp
Mahidol University
Phensuda Thaweephong
Mahidol University
Yusuke Miyata
Mahidol University

Research Article

Keywords: 3D printing, transtibial socket, additive manufacturing, PLA, digital workflow

Posted Date: June 1st, 2026

DOI: https://doi.org/10.21203/rs.3.rs-9722869/v1

License: This work is licensed under a Creative Commons Attribution 4.0 International License. Read Full License

Additional Declarations: No competing interests reported.

Abstract

Background

Conventional transtibial socket fabrication is a labor-intensive process that requires technical expertise, high cost, and long production times. This technical note presents a novel technique that integrates socket impression, smartphone-based 3D scanning, CAD modeling, and additive manufacturing to simplify socket fabrication and improve reproducibility.

Methods

17 resin sockets were duplicated using alginate and scanned using a smartphone TrueDepth sensor to create templates for digital modification. The sockets were modified in Blender and printed with tough PLA at 60% gyroid infill and 5 mm wall thickness. Clinical evaluation was conducted with 15 successfully delivered sockets to assess comfort and durability over three months.

Results

Out of 17 participants, 13 completed the one-month follow-up, and 7 completed the full three-month follow-up. The 3D-printed sockets achieved an average socket comfort score (SCS) of 8.60 ± 0.80, comparable to traditional resin sockets at 8.60 ± 0.54. Participants reported lighter socket weight and improved walking speed. However, a 50% structural failure rate within one month suggests that 60% infill may only be appropriate for temporary use. Higher densities must be prioritized in definitive socket applications.

Conclusion

This protocol demonstrates that 3D printing is a feasible, cost-effective alternative for transtibial socket fabrication, with the potential to improve accessibility and production efficiency without compromising anatomical fit. However, stronger material configurations are recommended for more durable sockets in the long term.

1. INTRODUCTION

Lower limb amputation represents a major global health challenge, with transtibial amputation being the most common [1, 2]. Primary causes include diabetes mellitus and peripheral arterial disease and traumatic injuries [1–4]. Functional ambulation with stability and comfort for the lost body part is achieved using a well-fitted prosthesis, where sockets play a pivotal role [5]. The prosthetic socket facilitates effective transmission of body weight and even pressure distribution across the residual limb while preventing skin breakdown and promoting long-term prosthetic use [5–7].

The conventional socket fabrication relies on a series of manual processes that can be time-consuming and labor-intensive, requiring expertise from prosthetists [8–9]. Variability between fabrication sessions and skills can also make it challenging to reproduce the same socket shape and fit consistently [10]. Furthermore, access to prosthetic care can be restricted due to limited certified prosthetists [11].

Advances in 3D printing technology have introduced alternative options in prosthetic socket fabrication. Fused deposition modeling (FDM), a form of additive manufacturing, allows complex or patient-specific sockets to be produced from digital designs with lower cost and less time, by 41.7% in transradial socket cases [12]. 3D printing also improves reproducibility since the designed file can be saved and reprinted consistently [9, 13].

Polylactic acid (PLA) is one of the most widely used filaments in FDM for transtibial socket printing due to its affordability, good strength-to-weight ratio, minimal warping, and ease of printing [13–17]. However, standard PLA can be brittle and prone to creep under sustained stress [14, 18]. Tough PLA, a modified derivative of PLA, offers improved toughness and impact resistance while retaining standard PLA properties (such as a low thermal expansion coefficient), rendering it viable for prosthetic applications [19–21]. Several studies have also used tough PLA for transtibial sockets due to its balance between printability, structural strength, and clinical practicality [22–25].

Despite the properties, there are limited technical protocols for the 3D-printed transtibial fabrication from residual-limb scanning to CAD-based socket design, and printing parameters. This technical note aimed to describe the complete workflow of designing and fabricating tough PLA sockets, along with clinical use in 15 transtibial amputees. We hope to inform clinicians and other interested stakeholders about the feasibility of adopting 3D printing for future prosthetic practice.

2. METHODS

2.1 Assessment

A total of seventeen participants received 3D-printed transtibial prostheses and were evaluated for immediate use, 1-month, and 3-month follow-ups. All participants underwent an assessment to confirm eligibility following the inclusion criteria: age between 18 and 65 years at the time of enrollment; unilateral transtibial amputation; functional level (K-level) of K3 or above (unlimited community ambulator: able to traverse most environmental barriers and can walk with variable cadence); non-primary amputee to prevent residual limb volume change; and no signs of skin breakdown or edema. This research, conducted

at the Sirindhorn School of Prosthetics and Orthotics, Bangkok, Thailand, has received ethical approval from the Siriraj Institutional Review Board (SIRB), no. 1038/2567, under Certificate of Approval (COA) no. 080/2025. Clinical Trial Registration was done retrospectively; TCTR20260514002. All participants have received detailed explanations of the study procedures, including the potential risks, and provided written informed consent before enrollment. The overall process for the recipient of both the traditional and 3D-printed socket in this study consisted of six phases (Fig. 1).

2.2 Socket duplication and 3D scanning

2.2.1 Socket duplication

This technical note uses the participant's current traditional socket as a template for a 3D-printed socket model. This approach ensures that the inner geometry remains consistent with the current socket, allowing the use of the same liner and minimizing adaptation to the new socket. Clinicians duplicated the resin socket using alginate, a biomaterial used in biomedical applications for its cost-effectiveness and dimensional accuracy [26–27]. Firstly, the current prosthesis was wrapped with plastic film for protection. The proximal brim of the resin socket was extended by about 2–3 cm using Plaster of Paris (POP) slab bandages to ensure complete capture of the inner socket surface, including the proximal aspect.

Alginate was prepared as a ratio of about 1:2 alginate powder to water, following the manufacturer's specifications. It was mixed with room-temperature water and stirred vigorously for approximately 1 minute, or until the mixture became homogeneous with no air bubbles. The mixture was poured into the socket, with a central pipe positioned to serve as a holder for the positive mold (Fig. 2A). Once the alginate sets, it becomes more viscous (Fig. 2B), the duplicated mold was removed from the socket and wrapped with 3–4 layers of Plaster of Paris (POP) slab bandage to get a rigid negative cast (Fig. 2C). During this stage, the alginate impression should remain moist since shrinkage can occur if the impression dries out, severely reducing overall circumference and volume. The POP cast is removed from the alginate mold and poured with plaster to get a positive model that is a replica of the current socket's interior surface. (Fig. 2D). The plaster is then smoothed with a wire and a brass net to prepare for 3D scanning (Fig. 2E).

While direct 3D scanning of the residual limb is becoming common, the use of an alginate-to-plaster transition was utilized here to provide a physical impression of the patient's current socket shape and dimensions. The plaster positive mold was then digitized using a 3D scanner. This hybrid approach ensures that the high-resolution surface details captured by the alginate are preserved, providing an intimate fit for the final 3D-printed socket based on a replica of the patient's current socket. The reference points for digital modification were drawn onto the plaster model, especially at PTB level, socket alignment, and circumferences, before scanning.

2.2.2 3D scanning

The smoothed plaster model was scanned using the smartphone application EM3D Scanner by Ethan Makes (Brawny Lads, USA). The application uses the TrueDepth camera sensor integrated into the iOS front camera to capture a depth map by projecting infrared dots onto the object's surface and generating a mesh that forms a 3D model [28–29]. The use of EM3D can further improve accessibility and enhance the production of 3D-printed sockets, as the scanner is embedded in mobile phones, which are portable and cheaper than handheld 3D scanners.

To optimize the TrueDepth camera from EM3D, the plaster model surface should be smooth and dry to reduce light scatter. The model is mounted vertically or horizontally on a bench vise to allow a 360-degree unobstructed view for the camera. Any unwanted objects are removed from the camera's field of view to ensure the sensor focuses only on the socket model. The phone is held parallel to the surface of the scanned model at a distance of about 25 cm to 30 cm, ensuring that the entire socket is captured within the camera's field of view. The user then slowly orbits the camera around the model and moves in upward and downward directions to capture the distal part or the proximal brim, respectively. An overlap between captured frames is recommended to make the EM3D application generate the depth map properly. The process may take a few minutes and some retries if the sensor loses tracking, which generally occurs with scanning an almost round or cylindrical object model. Once the scan is completed, a 3D file output is shown in (Fig. 2G), which can be exported as an STL or OBJ file for continued processing on Blender or other CAD software (Fig. 2H).

A direct scan on the residual limb can also be performed. The participant is seated with the knee joint in slight flexion, similar to traditional casting. The plastic film is wrapped around the stump to bind the soft tissue, and landmarks are drawn to identify pressure point areas as references in CAD. The measurements were recorded as a baseline and marked on the stump, including the residual limb length, circumferences, and mediolateral (ML) diameter at the supracondylar area (for PTB-SC socket). The process can be performed with or without the liner. However, if the scan is conducted without the liner, the 3D model must be scaled later on to accommodate the increased liner thickness.

The socket design process was performed on specialized software designed for prosthetic and orthotic modeling in Blender. The design workflow was executed as follows.

2.3 3D modelling in software

2.3.1 Socket model preparation

The scanned file (.obj) was imported into Blender 4.2.1. Initial processing involved anatomical marking of the patellar tendon and the removal of unwanted geometry to isolate the functional socket surface for modification. The socket was then positioned following the pre-drawn alignment in all coronal, sagittal, and transverse planes to replicate the patient's alignment as shown in Figs. 3.1A–3.1C. The software will then automatically calculate circumferences at every 2 cm, 3 cm, or 4 cm interval (depending on the measurement preferences) distal to the designated PTB level (Fig. 3.2).

2.3.2 Digital modification / Sculpting

Following this stage, the software will allow localized modifications. Areas for pressure points can be highlighted and selected to either build up relief over pressure-sensitive areas (bony prominences and distal end) or reduce pressure-tolerant areas (PTB, medial tibial flare, and popliteal fossa), following the principle [30] illustrated in Fig. 3.3. Since this study used a copied plaster model as a template for scanning, modifications were not necessary or performed minimally to maintain the same degree of relief and compression as the resin socket. Modifications were performed using a sculpting tool, allowing for precise control by labeling depth (mm) and area of influence (radius).

2.3.3 Defining the trimline and scaling

After sculpting, the user needs to label the proximal trimline so the software can cut it out into a socket model. The scanned socket can occasionally appear smaller than its actual size due to several confounding factors, such as alginate shrinkage, the position of the scanning camera, or errors in mesh generation. If the calculated circumferences do not match, the geometry scale can be adjusted to bring the volume as close as possible to the actual value. In this technical note, a baseline thickness of 5 mm was used for patients with standard weight and less impact activity. For patients with higher weight or work demands, the thickness was increased to 6 mm. To compensate for the strength of tough PLA, an additional 2 mm thickness was added to high-stress zones reported in previous studies, including the posteromedial brim (Fig. 3.7A), proximal trimline, and distal end [15, 16, 22, and 31].

2.3.4 Adapter attachment

The distal adapter template was imported into the software and positioned to align with the socket and foot alignment. Afterwards, the connection was used to create a seamless transition between the socket and the adapter base. A smooth transition can help reduce concentrated stress in the area, as a sharp angle at the distal end is most likely the point of structural failure.

2.4 3D printed manufacturing

2.4.1 Printing configurations

All 17 prosthetic sockets were printed using Creality 3D Filament Ender PLA+ filament and a Creality K2 Plus 3D printer (Creality Technology Co., Ltd., Shenzhen, China). Creality Print 7.0 was used as slicing software (Fig. 4A). The printing configurations were set according to the manufacturer's recommendation. All sockets were fabricated under the same slicer parameters as described in Table 1.

Table 1
Printing configurations set in the slicer program

Material	**Creality Ender PLA + 1.75 mm.**
Infill percentage	60% (32)
Infill pattern	Gyroid (33, 34)
Base thickness	5 mm (6 mm for high-weight patients) Additional thickness of 2 mm on corrugation areas
Layer height	0.2 mm.
Nozzle diameter	0.4 mm.
Nozzle temperature	220°C
Bed temperature	45°C
Printing speed	80 mm/s

The printing duration and material consumption for all sockets were 12.51 ± 2.73 hours and used 445.59 ± 85.43 g, respectively. PTB-SC sockets took 13.77 ± 2.96 hours and 475.63 ± 85.63 g, whereas PTB with a cuff strap suspension design took 11.40 ± 2.07 hours and 418.89 ± 80.47 g. Variations in total printing time across sockets were primarily due to differences in residual limb volume among participants, as larger residual limbs required greater print volume and number of layers. Secondary factors included socket design type, since the PTB-SC socket requires a higher proximal brim height than the standard PTB design to encompass the femoral condyle for anatomical suspension.

2.5 Fabrication and assembly

2.5.1 Attachment of the metal plate for the adapter

The plate adapter was attached to the 3D-printed socket by aligning it with the pre-designed holes at the distal end (Fig. 5A). A 5 mm-thick aluminum sheet was cut with a metal-cutting saw into 5x5 cm square pieces to serve as additional reinforcement between the adapter and the internal socket structure (Fig. 5B), further reducing the stress and preventing cracking at the distal end holes. Four holes were drilled into the aluminum sheet with a 5 mm drill bit, then tapped to accommodate 5 mm screws for secure fixation. The four-hole adapter was installed to align with the holes in the socket and the metal plate. The screws were then inserted and tightened to connect all components (Fig. 5C).

2.5.2 Attachment of the cuff strap suspension

A cuff strap suspension was attached to the PTB socket using a mechanical fastening technique. Two attachment points were identified and marked in the posteromedial and posterolateral regions following the standard anatomical positions for the cuff strap in the PTB socket design.

Pilot holes were drilled at each attachment point using a hand drill to match the screw diameter. A shallow groove matching the nut plate outline was created on the inner socket using a rasp head. The groove was heated, and the nut plate was pressed into the softened surface until flush with the inner wall. The plate was held in place until the material cooled, securing the nut plate in a heat-set configuration against the socket wall (Fig. 5D). The cuff strap was then attached using screws inserted through the pre-drilled holes from outside.

With automated 3D printing, the sockets can be produced within a single working day after CAD completion without requiring a clinician's presence during the printing. This provides an advantage over conventional fabrication methods, which typically require approximately two weeks in a clinic from casting to final delivery.

2.5.3 Component Assembly

The prosthetic foot and pylon heights were selected to match the current prosthetic prescription. The pyramid adapter, pylon, pylon adapter, and foot adapter were all ordered from Orto Centrum (Orto Centrum Ltd., Thailand) (Fig. 5E).

3. RESULTS

3D-printed prostheses were fitted and evaluated to ensure socket fit and alignment similar to that of participants' current prostheses. Participant-reported outcomes, performance tests, and biomechanical evaluations were conducted immediately after delivery of the 3D-printed prostheses, one-month follow-up, and three-month follow-up. However, this report focuses only on the participant-reported outcomes, fitting outcomes, and usage reports.

3.1 Participant demographic report

The average age was 52.94 ± 7.13 years, and the average weight was 65.12 ± 10.58 kg. All participants were classified K3-K4. The 3D-printed socket was designed based on the participant's current prosthetic design as described in Table 2.

18 participants were recruited following the inclusion criteria. One was excluded due to a distal-end ulcer. 17 sockets were fitted, and 15 (88.2%) were successfully delivered for long-term use. Only 7 participants (35.3%) had completed the full three-month follow-up, while the remaining had not yet reached this milestone. One participant was lost to follow-up after one month (Table 3).

Table 2
Report of participants' demographics of transtibial participants

Case	Age	Sex	Weight	K-Level	L/R[a]	Stump length (cm)[b]		Stump Shape[c]	Current Design[d]	Liner	Suspension type	Prosthetic foot
1	38	M	68	K4	L	21.0	M	V	endo	PE-lite	PTB Cuff	SACH
2	59	M	93	K3	L	16.5	M	U	exo	Derma Seal	PTB-SC	Single Axis
3	51	M	50	K3	R	21.3	M	V	exo	PE-lite	PTB-SC	SACH
4	54	M	80	K4	R	16.5	M	U	endo	PE-lite	PTB Cuff	SACH
5	48	M	66	K3	R	12.0	M	V	endo	PE-lite	PTB Cuff	Single Axis
6	67*	M	71	K4	R	24.0	L	U	endo	PE-lite	PTB Cuff	SACH
7	53	M	80	K3	R	13.7	M	V	endo	PE-lite	PTB-SC + knee sleeve	Single Axis
8	62	M	63	K3	R	16.2	M	V	endo	PE-lite	PTB Cuff	Single Axis
9	51	M	71	K4	L	20.0	M	V	exo	PE-lite	PTB Cuff	SACH
10	49	F	58	K4	L	14.5	M	U	endo	PE-lite	PTB SC	SACH
11	36	M	45	K3	R	19.0	M	V	endo	PE-lite	PTB-SC	Single Axis
12	37	M	49	K3	R	15.5	L	U	endo	PE-lite	PTB Cuff	SACH
13	59	M	71	K3	R	18.9	M	U	exo	PE-lite	PTB Cuff	SACH
14	66	M	57	K3	L	18.0	M	V	endo	PE-lite	PTB-SC	Single Axis
15	56	M	58	K3	L	12.5	M	U	endo	PE-lite	PTB Cuff	SACH
16	56	M	76	K3	R	31.5	L	V	endo	PE-lite	PTB Cuff	Single Axis
17	58	M	51	K3	R	16.8	M	V	endo	PE-lite	PTB-SC	SACH

*[a] Amputated side, [b] Stump length classification (M = medium, L = long), [c] Stump shape (V = conical shape, U = cylindrical shape), [d] Current prosthesis design (endo = endoskeletal, exo = exoskeletal) * The participant received a waiver*

Table 3
Summary of case events through the recruitment process to the last follow-up

Case	Day 1	Day 2	Day 3	Day 4
	Assessment and scanning	**Socket fitting**	**1-month follow-up**	**3-month follow-up**
1	✓	✓ Excessive toe-in	✓ Socket break	X[a]
2	✓	✓ Proximal ML looseness	✓	✓
3	✓	✓	✓	✓
4	✓	✓ Forefoot loading with posterior pylon lean	X[b]	X[b]
5	✓	✓ Too wide ML diameter, too long socket length	✓ Socket break	X[a]
6	✓	✓ Socket breaks at the screw Audible air sound	X[a]	X[a]
7	✓	✓ Excessive socket flexion	✓	✓
8	✓	✓ Proximal ML looseness	✓	✓
9	✓	✓ Excessive socket extension with a forefoot gap	✓	X[b]
10	✓	✓ Excessive socket extension with a forefoot gap	X[c]	X[c]
11	✓	✓	✓	✓
12	✓	✓ Excessive toe-in	✓	X[b]
13	✓	✓	✓	X[b]
14	✓	✓ Audible air sound Proximal ML looseness	✓	✓
15	✓	✓	✓	X[b]
16	✓	Excluded (unable to fit)	X[d]	X[d]
17	✓	✓	✓	✓
18	Excluded (wound ulcer)	X[d]	X[d]	X[d]
Remaining	**n = 17**	**n = 15**	**n = 13**	**n = 7**

[a] Stopped data collection after the 3D-printed socket broke, [b] Appointment fell after reported date,[c] Did not show up on the appointment date,[d] Excluded.

3.2 Individual socket adjustment and fitting result

During initial fitting, certified prosthetists performed alignment corrections until good alignment was achieved (Table 4 and Fig. 6). Excessive toe-in was identified in two patients (Cases 1 and 12) and was corrected by externally rotating the foot. Case 7 showed excessive socket flexion, while Cases 09 and 10 presented with excessive socket extension, with a forefoot gap, and were resolved with alignment adjustments. Forefoot loading with posterior pylon lean was observed in Case 4, caused by a soft heel bumper. A firm foam heel pad was added under the prosthetic foot to slightly tilt the prosthesis forward and reduce the plantar flexion moment.

Sockets in cases 06 and 14 had an audible air sound during the stance phase, likely due to a slightly loose fit and the mismatch between residual limb length and the original resin socket. Case 5 required adjusting the mediolateral diameter of the proximal brim by heating and compressing the socket wing.

Case 16

presented a unique fabrication challenge due to an extremely long transtibial residual limb that exceeded the printer's build volume (350 × 350 × 350 mm). The socket model was bisected into two segments in Blender and fused after printing using the heated filament. However, the lower-half segment became too narrow after applying heat, and the patient could not don it properly. Ultimately, the socket was not delivered, highlighting a current limitation of FDM printing for patients with long residual limbs.

During fitting, 4 out of 17 sockets had a mediolateral discrepancy at the proximal brim region, presenting approximately a 0.5 cm gap. The external brim surface was heated until malleable and manually adjusted. The socket was held in position until cooled, and then the adjusted diameter was re-evaluated. However, this technique should be used cautiously, as excessive or uneven heating may cause material distortion or unintended softening of adjacent regions. Reprinting is preferable in case major adjustments are required.

Most participants reported easy adaptation because the internal shape of the alginate-duplicated socket closely resembled their existing socket. Skin inspection after gait showed no signs of pressure sores, redness, or pain associated with the residual limb adapting to a new prosthesis.

Table 4
Report of individual adjustment during 3D modeling process and fitting result

Case	Individual adjustment					Printing properties		Fitting result
	Printed scale (mm)	Wall thickness (mm)	Brim thickness (mm)	Posterior medial brim corrugation	Base corrugation	Print time (hr)	Material used (g)	
1	2.5	5	2	-	-	12.35	444	Good fit
2	3.5	6	3	✓	-	16.72	642	Loose
3	2.5	5	2	-	-	13.62	506	Good fit
4	2.5	5	2	✓	-	14.78	543	Good fit
5	3.0	5	2	✓	✓	9.55	342	Good fit
6*	2.5	5	2	-	-	13.15	515	Loose
7	2.5	5	2	-	-	13.05	432	Good fit
8	2.5	5	2	-	-	9.98	367	Good fit
9	2.5	5	2	-	-	11.40	424	Good fit
10	2.5	5	2	-	-	11.00	378	Good fit
11	3.0	5	2	-	-	12.37	454	Good fit
12	2.5	5	2	-	-	10.88	389	Good fit
13	3.5	5	2	-	-	12.53	453	Loose
14	3.0	5	2	-	-	12.90	449	Tight
15	2.5	5	2	✓	-	7.95	293	Good fit
16*	2.5	5	2	-	-	19.58	543	Tight
17	3.0	5	2	-	-	10.93	401	Good fit

**Did not deliver the 3D-printed socket prosthesis*

3.3 Long-term usage

After delivery, 7 sockets (41.2%) experienced structural failure after 1 month (Table 5). Fracture points were identified at two locations: the posteromedial brim, recorded in 4 sockets (23.5%) (Fig. 7A), and base fractures, recorded in 3 sockets (17.6%): 2 cases around the connection area (Fig. 7B) and 1 case at the posterior screw holes of the adapter (Fig. 7C).

Table 5
Socket failure summary (N = 16, excluding the socket that did not pass fitting)

Fracture location	No. of cases (N = 16)	Duration of fracture	Usage		Outcome	Follow-up status
			Indoors	Outdoors		
Posteromedial brim	4 (25%)	1 week and 11 weeks (1 case)	✓	✓	Repair with the PLA+ filament welding technique	3 months follow-up completed
		1 month (1 case)	✓	✓		
		2 months (1 case)	✓	✓		
		Fitting day and 5 weeks (1 case)	✓	✓	PLA welding and self-modification by the participant using sawdust	
Adapter interface	2 (12.5%)	Fitting day (1 case)*	✓	✓	Reinforce with Scotch® cast and reprint a new socket	Immediate outcome only
		1 month (1 case)	✓	✓		Completed only 1 month follow-up
Connection area	2 (12.5%)	1 month (2 cases)	✓	✓		
Total fractures	8 (50%)					
No fracture	8 (50%)					

*Note: All sockets that had structural failure were printed with 60% infill and 5 mm wall thickness. *Not delivered for use*

Cracks along the posteromedial brim were temporarily fixed using tough PLA filament. A piece of filament was melted with a heat gun and sealed along the crack area (Fig. 7A). Sockets that failed at the connection area were reinforced with Scotch® cast (Fig. 7B). The affected socket files were subsequently reprinted with additional corrugation or higher infill percentages to improve structural strength and reduce the risks of repeated failure.

Case 6

was the only case that had a breakage during the immediate outcome fitting. The filament around two posterior screws disconnected from the base of the adapter, and the socket was not ultimately delivered (Fig. 7C)

At the time of reporting, 7 sockets passed the 3-month follow-up (including 4 sockets that previously developed medial brim cracks and were repaired with tough PLA welding). Self-reported daily usage time varied depending on activity level, environment, and socket tolerance. Five participants reported near full-day use for both indoors and outdoors (Cases 05, 07, 11, 14, and 17), while Case 11 used the 3D-printed socket instead of the resin socket for most activities.

Several patients (Cases 02, 03, 08, 09, 13, and 15) restricted use mainly to indoor ambulation due to the absence of cosmetic foam covering, work-related activities, and a preference for a more durable exoskeletal prosthesis for outdoor use.

3.4 Socket Comfort score

Socket Comfort Score (SCS) data is reported in Table 6. Mean comfort scores were comparable between the resin (8.60 ± 0.54) and 3D-printed socket (8.60 ± 0.80). Several participants reported that the 3D-printed socket felt lighter than their traditional resin socket, which was reflected in higher or equivalent SCS scores in multiple cases.

Table 6
Report of the socket comfort score, compared between the traditional resin socket and the 3D-printed socket after fitting

Case	Resin Socket	3D Socket	Notes for 3D-printed socket
01	9/10	9/10	Comparable comfort
02	8/10	8/10	Comparable comfort
03	9/10	10/10	Lighter than a resin socket and no excessive sweating
04	8/10	8/10	Similar comfort; alignment differs due to a soft bumper
05	8/10	7/10	Felt the 3D socket weight was concentrated at the distal end
06	N/A	N/A	Not delivered
07	9/10	8/10	Alignment differs; 3D socket in excessive flexion
08	8/10	7/10	Reported lack of confidence in the 3D socket
09	8/10	9/10	The 3D socket was lighter and more comfortable
10	8/10	8/10	The 3D socket was lighter and well-fitted
11	9/10	10/10	Preferred 3D over resin socket (full-time use)
12	8/10	9/10	Reported lightweight and faster walking with a 3D socket
13	10/10	10/10	Slightly loose but provided similar comfort
14	9/10	8/10	Distal tightness and proximal ML looseness
15	9/10	9/10	Well-fitted; patient preferred looser socket with multiple socks
16	N/A	N/A	Not delivered
17	9/10	9/10	Lighter weight and better gait; concerned about strength

4. DISCUSSION

4.1 Scanning accuracy and socket fitting

A 70.59% success rate (12 of 17 cases) for initial fitting without adjustment suggests that combining alginate socket impressions with smartphone-based 3D scanning is a viable alternative to traditional casting. By using the current socket as a template, the socket volume and internal geometry can be replicated into positive casts. Smartphone-based direct photogrammetry was reported to achieve higher accuracy when scanned on positive casts, up to 99.13%, than scanning the internal socket walls at 38.37% [35]. The clinical viability of smartphone-based scans is further supported by the findings of Kaul et al. (2024), demonstrating that the scan quality and completeness from EM3D are comparable to those of EinScan and validating its use as an alternative option for 3D scanning [28]. However, discrepancies in proximal mediolateral diameter and overall socket fit suggest that errors can still occur during this process.

5 cases (29.41%) had socket-fitting issues: 3 sockets had an overall looseness, and 2 cases presented tightness at the distal region along with a proximal ML gap. The overall looseness or tightness of the socket may have resulted from several confounding factors, such as 1) alginate shrinkage during plaster cast capture, which reduces the overall circumference; 2) mesh generation error after the initial scan; and 3) scaling inaccuracy by the clinician.

Clinical solutions are varied. The loose socket was accommodated by increasing 1–2 layers of stump socks. Meanwhile, the tight socket was attempted by heating and expanding. Although heating adjustments have been reported in some studies to help address these issues [36–37], the method is highly sensitive and should be performed cautiously. Due to PLA's low glass transition temperature, non-uniform or excessive heating can cause material distortion and layer delamination, compromising structural integrity and volume. This technique is more suitable for minor pressure relief over specific areas. If a major adjustment of the socket is needed, it is better to reprint with a new scale or a new digital modification.

Improper smartphone position can cause mesh errors and volume inaccuracies. If the phone is not held parallel to the model surface, the generated mesh may be distorted, resulting in a loose proximal ML and distal tightness, as observed in 3 cases. In addition, the distance between the stump and the smartphone camera may contribute to scaling errors. Ideally, maintain 30 cm from the model to maximize the linear and angular trueness of the model during the scan [38–39]. Uniform lighting can also affect the quality of the scan, especially if the scan is taken with a residual limb. Shadowed posterior regions of the stump may provide fewer identifiable features for tracking, leading to surface irregularities during the scan [40].

4.2 Participant-reported outcomes

During fitting, the 3D-printed sockets achieved a Socket Comfort Score (SCS) of 8.60 ± 0.80, comparable to that of traditional resin sockets (8.60 ± 0.54). The primary advantage reported by participants was the weight reduction, which was associated with increased walking speed, faster swing length, and reduced fatigue. Similarly, the findings by Eshraghi et al. (2024) reported the SCS for traditional and 3D-printed sockets at 8.3 ± 0.5 and 7.8 ± 1.6, respectively [9]. Additionally, it was reported that digital scanning reduces the time by 34% compared to traditional casting, with participants reporting 7.45%

greater satisfaction with digital scanning than plaster casting [9]. The subjective preference for lightweight sockets implies the potential of 3D printing applications to improve quality of life. However, the material strength remains a concern for outdoor and high-impact usage. Once resolved, 3D printing can be used to manufacture prosthetic sockets that are well-contoured and lightweight more quickly.

4.3 Structural failures and durability concerns

The primary challenge in this study was the high rate of structural failure (50%) after one month of use. Fractures were mainly found in two high-stress zones: the posteromedial brim (25%) and the distal adapter base (25%), as reported in several studies [16, 22–23, 32, 41–42]. Fractures at the posteromedial brim likely result from the bending moments and shear forces during late stance. Our attempts to reinforce these areas with PLA filament welding or by adding 2 mm of corrugation to the brim provided only temporary fixes. However, these techniques did not prevent secondary fractures proximal to the previous crack site in two cases, suggesting that localized thickening warrants further investigation and optimization with different infill percentages, patterns, or base materials.

The second point of failure was at the adapter connection at the distal end, which occurred during terminal stance. This issue is likely due to stress concentrations at the square-shaped transition zones. The sharp angle can act as a notch, resulting in crack propagation parallel to the printing direction. The brittleness of PLA can also cause delamination between adjacent layers. In this study, the failure at the distal end propagates above the aluminum reinforcement plate. Further optimization should implement circular transitions at the distal end to help distribute loads more evenly, or a selective wall pattern and thickness targeting the distal end zone. Combining other materials (such as carbon fiber or cement) with a 3D-printed base socket has been reported to improve overall strength and yield strength by 89.57%, suggesting that multi-material reinforcement is effective for enhancing socket durability. [24]

4.4 Infill density strength

The infill percentage was set at 60% based on evidence from Fadzil et al. (2020), in which the effects of different infill percentages (20%, 40%, 60%, and 100%) on 3DP socket strength were evaluated using finite element analysis (FEA) and cyclic tests under 600 N load. Their study concluded that the socket at 60% infill percentage was the most suitable density for PLA, as it has a lower value of total deformation, shear stress, and Von Mises stress with less time taken for printing (13 hr) than 80% (15 hr 14 min) or 100% infill (21 hr 15 min), as shown in Table 7 [32]. In this study, the 60% infill density was applied uniformly across the socket body.

Table 7
Structural Performance of PLA Sockets at Different Infill Densities, adapted from Wan Fadzil et al., 2020

Infill density (%)	Von Mises Stress (MPa)	Shear Stress (MPa)	Total deformation (mm)	Printing time	Material weight (g)
20	0.440	0.251	2.00	8 h 20 min	620
40	0.413	0.237	1.00	10 h 41 min	870
60 (selected)	**0.413**	**0.237**	**0.069**	**13 h 00 min**	**1125**
80	0.413	0.237	0.052	15 h 14 min	1378
100	0.413	0.237	0.041	21 h 15 min	1594

However, our clinical results demonstrate that 60% infill is insufficient for definitive, long-term ambulation, particularly for K3-K4 users. This aligns with recent findings by van der Stelt et al. (2025), who demonstrated that tough PLA with 100% infill is necessary to withstand 2.27 million loading cycles over 2.5 years of continuous use [43]. Although 60% infill may suffice for temporary diagnostic sockets, definitive sockets should prioritize 100% density to ensure patient safety and device longevity.

Infill percentage was identified by Ginting et al. (2026) as a more significant factor influencing the tensile strength ($p = 0.003$) than infill pattern ($p = 0.791$) or printing speed ($p = 0.154$) (44). Therefore, to further increase the strength of 3D-printed sockets, the infill density should be prioritized. Notably, a solid specimen with 100% infill achieved the highest tensile strength at 47.84 MPa, with a significant difference of approximately 16.56 MPa when changing from 50% to 100% infill [44–45]. Their studies could serve as a benchmark for prosthetic fabrication in future clinical trials.

4.5 Cost and clinical practicality

The digital workflow of CAD and 3D printing gives an advantage over traditional fabrication methods, reducing fabrication time from the traditional two-week period to a single working day. In our trials, the automated printing required an average of 12.51 ± 2.73 hours and consumed 445.59 ± 85.43 g. The total socket cost, excluding other components, is estimated at an average of 565 Baht per socket (PTB-SC at 573 Baht and PTB at 559 Baht) compared to a traditional resin socket (generally costs 3,000 Baht at SSPO).

Although further optimization is needed to improve long-term durability, the reduced cost, faster fabrication time, and acceptable comfort outcomes suggest that 3D-printed sockets may serve as a practical alternative for temporary or low-cost prosthetic provision in resource-limited settings

This study has several limitations. First, the sample size was relatively small, and not all participants completed the full three-month follow-up. Therefore, long-term evaluation of socket durability and usage is limited. Second, the sockets were fabricated using a single printing configuration (60% infill, gyroid pattern, and tough PLA material), which did not represent the optimal design for definitive prosthetic use. Moreover, variations in smartphone scanning technique, lighting conditions, and socket duplication methods may have affected scanning accuracy and socket fit, as shown in several fitting cases.

Finally, this technical note primarily focused on the fabrication method, fitting outcomes, and participant-reported results. Comprehensive biomechanical and long-term clinical evaluations are still required.

5. CONCLUSION

This technical note supports the feasibility of using 3D printing with tough PLA to manufacture transtibial prosthetic sockets. The digital workflow improves efficiency through automation, reducing both manufacturing costs and time. The printed sockets were also lighter in weight while maintaining contour and comfort, without causing skin breakdown or pain, as reflected by comparable SCS scores.

However, structural failures at the proximal brim and distal end indicate that durability is still insufficient for long-term use. Most sockets used outdoors failed either at the posteromedial brim or the distal area after at least 1 month of use. Some participants did not notice medial brim breakage until they returned home, which raises safety concerns and limits real-world applications. The current tough PLA socket design (60% infill, gyroid pattern, and 5 mm wall thickness) is therefore most appropriate for temporary use, indoor ambulation, or low-impact activities. Clinicians should be aware of the risk of material delamination under repetitive high-load cycles, especially beyond one month.

Further studies should investigate prosthetic sockets with higher infill (80–100%) or multi-material designs, combining tough PLA with other reinforced composites to strengthen high-stress regions, such as the distal end and posteromedial brim. Additionally, long-term studies beyond 6 months are required to establish the fabrication standards of 3D-printed definitive sockets under different loading conditions.

Declarations

Conflicts of Interest

The authors declare no conflicts of interest. The funders had no role in the study design, data analyses, or publication of the results.

Funding

This research project has been supported by Mahidol University (Fundamental Fund: fiscal year 2025 by National Science Research and Innovation Fund (NSRF)) (IO) R016841005.

Author Contribution

NM – Conceptualization, Methodology, Writing - Review & Editing, Supervision; PT – Conceptualization, Methodology, Resources, Writing - Review & Editing, Project administration, Funding acquisition; TN - Data Curation, Writing - Original Draft, YM – Methodology, Supervision

Acknowledgement

We want to express our appreciation to the main sponsor and to our team colleagues for their hard work from beginning to end. Special thanks to Ms. Yasmin Nutchumlong, Certified Prosthetist and Orthotist at Sirindhorn School of Prosthetics and Orthotics, Faculty of Medicine, Siriraj Hospital, Mahidol University, for her support during 3d socket prostheses fittings, and Ms.Sirarat Chaisumritchoke, for her cooperation and management at the beginning of this study. Unforgettable thanks to the volunteers who participated in this study.

Data Availability

Data sharing is not applicable to this article as no datasets were generated or analyzed during the current study.

References

1. T. Curtis, A.L. Adams, Below-Knee Amputation. National Library Med National Center Biotech Info, StatPearls Publishing (Jan 2024). Available from:https://www.ncbi.nlm.nih.gov/books/NBK534773/#:~:text=A%20below%2Dknee%20amputation%20(BKA,as%20a%20life%2Dsaving%20procedure
2. Gerasimos Bastas. Science Direct, Lower Limb Amputations. The Clinician's Handbook of natural Med (3rd edition), Essentials of Physical Med and Rehabilitation (4th Edition), 2020. Available from: https://www.sciencedirect.com/topics/medicine-and-dentistry/amputation-of-lower-limb
3. S. Ozkan, C. Adanas, The causes and levels of lower limb amputation in geriatric patients. Annals Med. Res. **28**, 893 (2021). 10.5455/annalsmedres.2020.05.508
4. C.L. McDonald, S. Westcott-McCoy, M.R. Weaver, Haagsma, Juanita3; Kartin, Deborah1. Global prevalence of traumatic non-fatal limb amputation. Prosthetics and Orthotics International 45(2):p 105–114, April 2021. | 10.1177/0309364620972258
5. P.M. Stevens, R.R. DePalma, S.R. Wurdeman et al., July t. Transtibial socket design, interface, and suspension: A clinical practice guideline. J Prosthet Orthot. 2019;31(3):172–178. Available from: http://dx.doi.org/10.1097/jpo.0000000000000219

6. L.E. Pezzin, T.R. Dillingham, E.J. MacKenzie, P. Ephraim, P. Rossbach, Use and satisfaction with prosthetic limb devices and related services. Arch. Phys. Med. Rehabil. **85**, 723–729 (2004). 10.1016/j.apmr.2003.06.002
7. L. Paterno, M. Ibrahimi, E. Gruppioni, A. Menciassi, L. Ricotti, Sockets for limb prostheses: A review of existing technologies and open challenges. IEEE Trans Biomed Eng [Internet]. 2018;65(9):1996–2010. Available from: http://dx.doi.org/10.1109/tbme.2017.2775100
8. L. Li, M. Miguel, C. Phillips, L. Verweel, M.B. Wasilewski, C. MacKay, A qualitative study exploring healthcare professionals' perceptions of lower limb 3D printed sockets. Disabil Rehabil [Internet]. 2024;46(17):4033–9. Available from: http://dx.doi.org/10.1080/09638288.2023.2258345
9. A. Eshraghi, C. Phillips, C. MacKay, S. Dilkas, Z. Riondato, S. Lehkyj, W. Heim, Comparison of socket geometry, socket comfort, and patient experience between manually- and digitally-designed prosthetic sockets for lower-limb amputees: A feasibility study. Prosthesis. **6**(3), 672–682 (2024). https://doi.org/10.3390/prosthesis6030048
10. M.R. Safari, P. Rowe, A. McFadyen, A. Buis, Hands-off and hands-on casting consistency of amputee below knee sockets using magnetic resonance imaging. TheScientificWorldJournal. **2013**(1), 486146 (2013). https://doi.org/10.1155/2013/486146
11. K. Jefferson, W. Rajah, Chericoff et al., t. Enabling Mobility: A Simulation Model of the Health Care System for Major Lower-Limb Amputees to Assess the Impact of Digital Prosthetics Services. System Models for Public Health and Health Care Policy. 2023(1). Available from: https://doi.org/10.3390/systems11010022
12. J. Olsen, S. Day, S. Dupan, K. Nazarpour, M. Dyson, 3D-printing and upper-limb prosthetic sockets: Promises and pitfalls. IEEE Trans. Neural Syst. Rehabil Eng. [Internet]. **29**, 527–535 (2021). http://dx.doi.org/10.1109/TNSRE.2021.3057984
13. S. Kim, S. Yalla, S. Shetty, N.J. Rosenblatt, 3D printed transtibial prosthetic sockets: A systematic review. PloS One. **17**(10), e0275161 (2022). https://doi.org/10.1371/journal.pone.0275161
14. V. Plesec, J. Humar, P. Dobnik-Dubrovski, G. Harih, (2023). Numerical analysis of a transtibial prosthesis socket using 3D-printed bio-based PLA. Materials, 16(5), 1985. https://doi.org/10.3390/ma16051985
15. D.F. Fitriyana, S. Palanisamy, Y.S. Wicaksana, S. Anis, J.P. Siregar, T. Cionita, K. Sureshkumar, A. Alagarsamy, N. Ayrilmis, M. Abbas, S. Kalathil, M.Z. Rahman, Mechanical performance analysis of a 3D printing-based transtibial prosthetic socket against the gait cycle using the finite element method. RSC Adv. **15**(30), 24150–24166 (2025). https://doi.org/10.1039/d5ra03155a
16. T. Marinopoulos, S. Li, V.V. Silberschmidt, Mechanical performance of 3D printed prosthetic sockets: An experimental and numerical study. Procedia Struct. Integr. **42**, 903–910 (2022). https://doi.org/10.1016/j.prostr.2022.12.114
17. A.J.R. Barcena, P. Ravi, S. Kundu, K. Tappa, Emerging biomedical and clinical applications of 3D-printed poly(lactic acid)-based devices and delivery systems. Bioeng. (Basel Switzerland). **11**(7), 705 (2024). https://doi.org/10.3390/bioengineering11070705
18. K. Tappa, U. Jammalamadaka, Novel biomaterials used in medical 3D printing techniques. J. Funct. Biomaterials. **9**(1), 17 (2018). https://doi.org/10.3390/jfb9010017
19. N. Naveed, Investigating the material properties and microstructural changes of fused filament fabricated PLA and tough-PLA parts. Polymers. **13**(9), 1487 (2021). https://doi.org/10.3390/polym13091487
20. K. Hashima, S. Nishitsuji, T. Inoue, Structure-properties of super-tough PLA alloy with excellent heat resistance. Polymer. **51**(17), 3934–3939 (2010). https://doi.org/10.1016/j.polymer.2010.06.045
21. N. Wu, H. Zhang, Mechanical properties and phase morphology of super-tough PLA/PBAT/EMA-GMA multicomponent blends. Mater. Lett. **192**, 17–20 (2017). https://doi.org/10.1016/j.matlet.2017.01.063
22. van der M. Stelt, F. Stenveld, T. Bitter, T.J.J. Maal, D. Janssen, Design evaluation of FFF-printed transtibial prosthetic sockets using follow-up and finite element analysis. Prosthesis. **4**(4), 589–599 (2022). https://doi.org/10.3390/prosthesis4040048
23. D.C. Wijnbergen, van der M. Stelt, L.M. Verhamme, The effect of annealing on deformation and mechanical strength of tough PLA and its application in 3D printed prosthetic sockets. Rapid Prototyp. J. **27**(11), 81–89 (2021). https://doi.org/10.1108/rpj-04-2021-0090
24. M.H. Ramlee, M.I. Ammarullah, M. Sukri, N.S.F. Hassan, N.S. Baharuddin, M. H., A. Kadir, M. R, Investigation on three-dimensional printed prosthetics leg sockets coated with different reinforcement materials: analysis on mechanical strength and microstructural. Sci. Rep. **14**(1), 6842 (2024). https://doi.org/10.1038/s41598-024-57454-8
25. R. Ginting, A. Ishak, F.R.P. Nasution, R. Silalahi, Innovative design of a transtibial prosthetic socket through integration of QFD, reverse engineering, and 3D printing. Manuf. Technol. **25**(6), 778–787 (2025). https://doi.org/10.21062/mft.2025.085
26. K.Y. Lee, D.J. Mooney, Alginate: properties and biomedical applications. Prog. Polym. Sci. **37**(1), 106–126 (2012). https://doi.org/10.1016/j.progpolymsci.2011.06.003
27. N. Naderi Geisour, H. Ariamanesh, M. Sheikhi, S. Pezeshki, M.M. Mohammadi, Dimensional accuracy of alginate mold method on duplication of stone casts. Casp. J. Dent. Res. **11**(2), 91–97 (2022). http://cjdr.ir/article-1-385-en.html
28. R. Darbari Kaul, C. Duong, J. Ma, S. Sayyar, G. Wallace, M. Dunn, K. Cheng, S. Fleming, S. Whereat, J. Clark, P. Mukherjee, A comparison of the accuracy and feasibility of a low-cost mobile application versus higher-cost handheld 3D scanner for digital ear prosthetics. ANZ J. Surg. **95**(4), 719–726 (2025). https://doi.org/10.1111/ans.19374
29. S. Barone, A. Antonelli, M. Salviati, V. Greco, F. Bennardo, K. Becker, A. Giudice, M. Simeone, Accuracy Assessment of EM3D App-Based 3D Facial Scanning Compared to Cone Beam Computed Tomography. Dentistry J. **12**(11), 342 (2024). https://doi.org/10.3390/dj12110342
30. A. Gitter, G. Bosker, *Physical Medicine and Rehabilitation: Principles and Practice, Physical Medicine and Rehabilitation: Principles and Practice*, ed. by J.A. DeLisa (Lippincott Williams & Wilkins, 2005), pp. 1326–1354

31. L. Campbell, A. Lau, B. Pousett, E. Janzen, S.U. Raschke, How infill percentage affects the ultimate strength of 3D-printed transtibial sockets during initial contact. Can. Prosthetics Orthot. J. **1**(2) (2018). https://doi.org/10.33137/cpoj.v1i2.30843
32. W.F.A.W. Fadzil, M.A. Mazlan, A.H. Abdullah, F.A. Hanapiah, A.I. Pangesty, Effects of Infill Density on 3D Printed Socket for Transtibial Prosthetic Leg. J. Mech. Eng. **9**(SpecialIssue1), 229–238 (2020)
33. H. Moeinnia, C. Ganzert, L. Schubert, W.S. Kim, Streamlined custom manufacturing for optimized 3D printed prostheses through 3D pressure mapping. Biosens. Bioelectron. **302**, 118560 (2026). 10.1016/j.bios.2026.118560
34. C. Silva, A. Pais, G. Caldas, B. Gouveia, Alves, Jorge, Belinha, Jorge, Study on 3D printing of gyroid-based structures for superior structural behaviour. Progress Additive Manuf. **6** (2021). 10.1007/s40964-021-00191-5
35. S. Cullen, R. Mackay, A. Mohagheghi, X. Du, The use of smartphone photogrammetry to digitise transtibial sockets: Optimisation of method and quantitative evaluation of suitability. Sens. (Basel Switzerland). **21**(24), 8405 (2021). https://doi.org/10.3390/s21248405
36. van der M. Stelt, M.P. Grobusch, A.R. Koroma, M. Papenburg, I. Kebbie, Masanga, C.H. Slump, T.J.J. Maal, L. Brouwers, Pioneering low-cost 3D-printed transtibial prosthetics to serve a rural population in Sierra Leone - an observational cohort study. EClinicalMedicine. **35**, 100874 (2021). PMID: 34027333; PMCID: PMC8129890
37. J. Olsen, S. Day, S. Dupan, K. Nazarpour, M. Dyson, 3D-printing and upper-limb prosthetic sockets: Promises and pitfalls. IEEE Trans. Neural Syst. Rehabil. Eng. **29**, 527–535 (2021). https://doi.org/10.1109/TNSRE.2021.3057984
38. J. Lee, C. Nkama, H. Yusuf, J. Maina, J. Ikuzwe, J. Byiringiro, M. Busogi, C. Tucker, (2025). Accessible digital reconstruction and mechanical prediction of 3D-printed prosthetics. Journal of Mechanical Design (New York, N.Y.: 1990), 147(6). https://doi.org/10.1115/1.4067716
39. M. Revilla-León, M. Gómez-Polo, M. Drone, A.B. Barmak, C. Guinot-Barona, W. Att, J.C. Kois, A. Pérez-Barquero, J, Impact of scanning distance on the accuracy of a photogrammetry system. J. Dent. **142**(104854), 104854 (2024). https://doi.org/10.1016/j.jdent.2024.104854
40. S. Walters, B. Metcalfe, M. Twiste, E. Seminati, N.Y. Bailey, Smartphone scanning is a reliable and accurate alternative to contemporary residual limb measurement techniques. PloS One. **19**(12), e0313542 (2024). https://doi.org/10.1371/journal.pone.0313542
41. L. Campbell, A. Lau, B. Pousett, E. Janzen, S.U. Raschke, How Infill Percentage Affects the Ultimate Strength of a 3D-Printed Transtibial Socket. Canadian Prosthetics & Orthotics Journal, Volume 1, Issue 2, 2018; Abstract, Poster Presentation at the AOPA's 101st National Assembly, Sept. 26–29, Vancouver, Canada, 2018. https://doi.org/10.33137/cpoj.v1i2.32038
42. E.A. Nickel, K.J. Barrons, M.K. Owen, B.D. Hand, A.H. Hansen, J.D. DesJardins, Strength testing of definitive transtibial prosthetic sockets made using 3D-printing technology. J. Prosthetics Orthot. **32**(4), 295–300 (2020). https://doi.org/10.1097/jpo.0000000000000294
43. van der M. Stelt, L. Brouwers, S. Jalloh, O. Kamara, M. Grobusch, T. Maal, R. Leijendekkers, Longevity and effectiveness of 3D-printed transtibial prosthetic sockets in rural Sierra Leone: A pilot study with 2.5-year follow-up. Prosthet. Orthot. Int. (2025). https://doi.org/10.1097/PXR.0000000000000465
44. R. Ginting, A. Ishak, F.R.P. Nasution, R. Silalahi, Influence of infill pattern on tensile strength and material efficiency of fused deposition modelling (FDM)-printed polylactic acid (PLA) parts. Int. J. Nanoelectronics Mater. (IJNeaM). **19**(2), 213–222 (2026)
45. R. Ginting, A. Ishak, F.R.P. Nasution, R. Silalahi, Innovative design of a transtibial prosthetic socket through integration of QFD, reverse engineering, and 3D printing. Manuf. Technol. **25**(6), 778–787 (2025). https://doi.org/10.21062/mft.2025.085

Figures

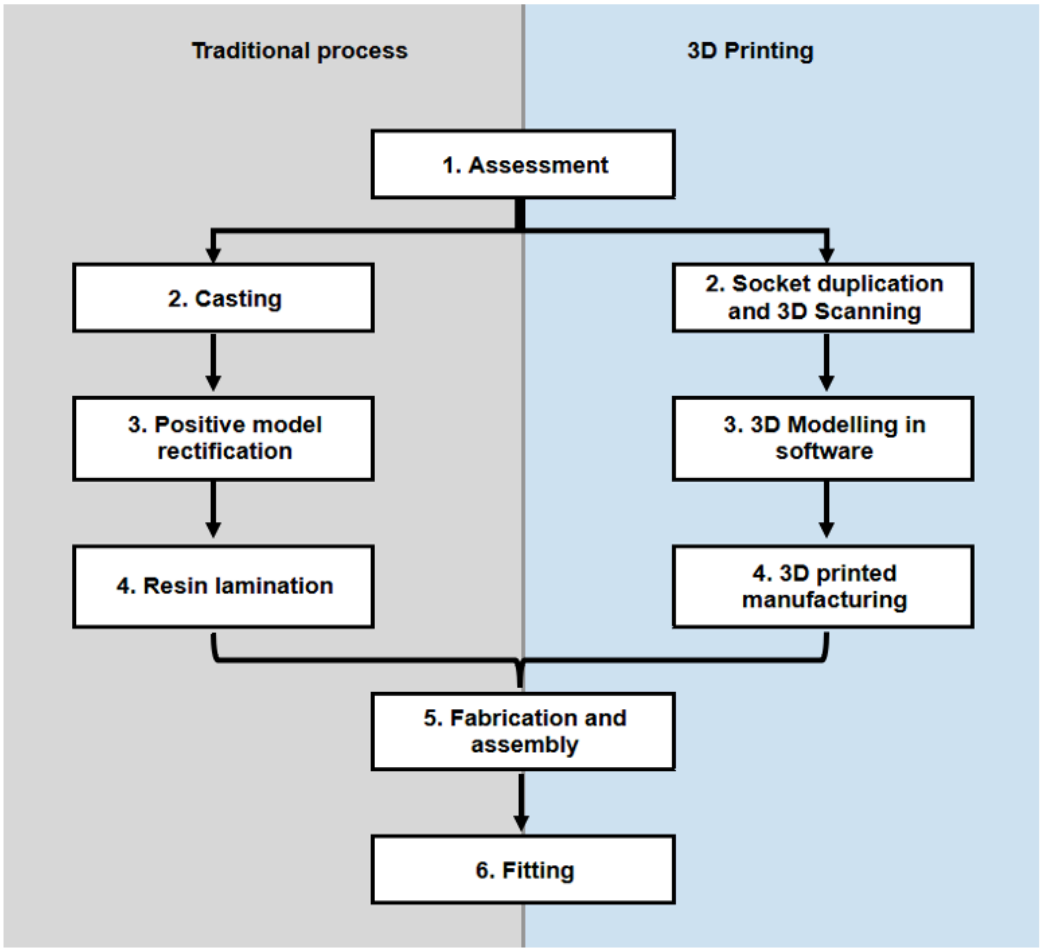


Figure 1

Comparison of the workflow between traditional and 3D-printed transtibial socket manufacturing

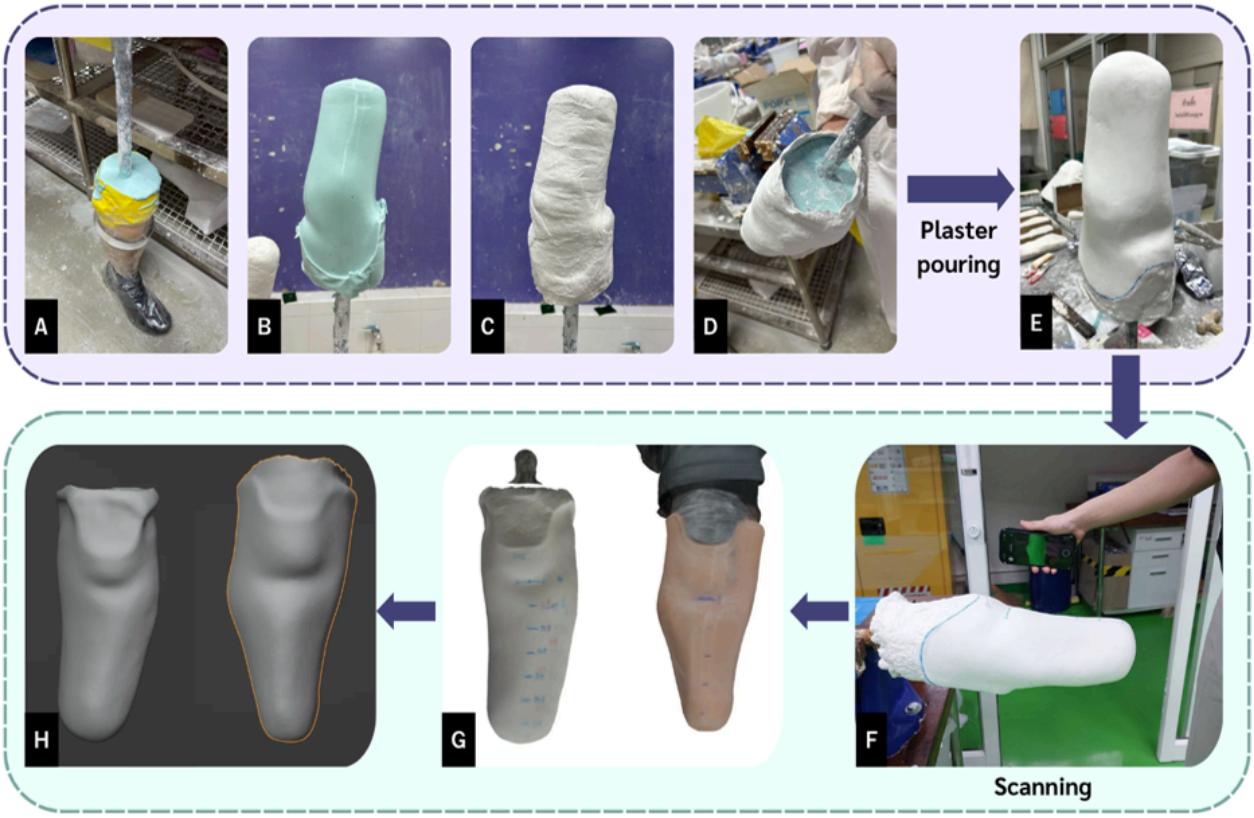


Figure 2

(A-E) Socket duplication process, (F) 3D scanning process, (G) Scanned model viewed in EM3D, (H) Imported socket mesh file in Blender



Figure 3

Overview of transtibial socket design in Blender. Alignment setup in transverse (1A), coronal (1B), and sagittal planes (1C), (2) Calculating the socket circumferences, (3) Modification of pressure-tolerant and pressure-sensitive areas following Gitter and Bosker in 2005 (30), (4) Socket length extension for bony residuum or if needed, (5) Trimline drawing and scaling, (6) Setting the base thickness; Additional thickness on posteromedial area (7A) and the proximal brim (7B), Socket adapter alignment setting in sagittal (8A) and coronal planes (8B), (9) Creating a transition between the socket and adapter, (10) Creating base corrugation before export

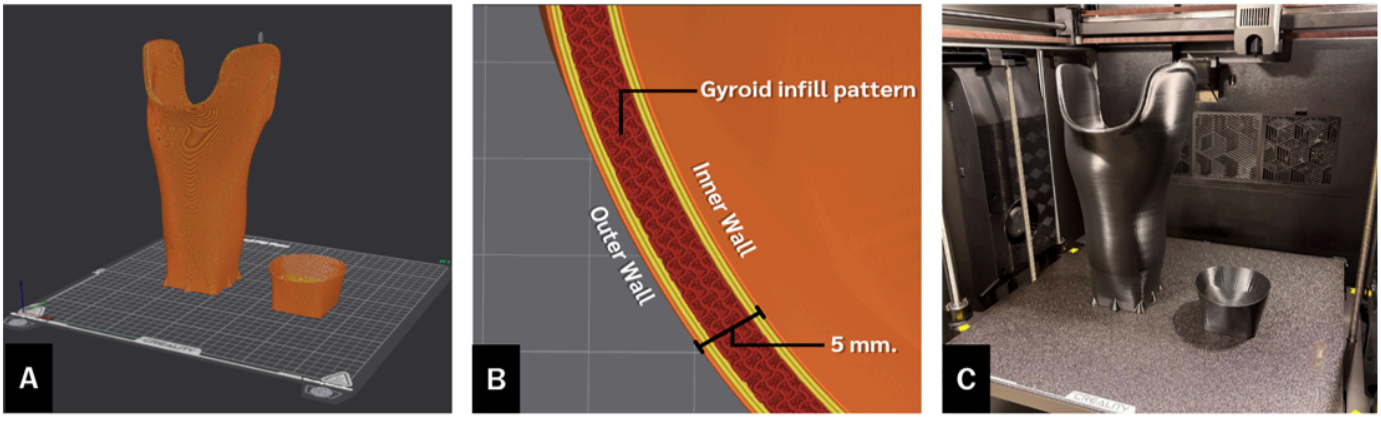


Figure 4

(A) PTB-SC socket viewed in Creality Print slicer, (B) cross-sectional view of the socket wall, (C) the printed socket in Creality K2 Plus printer

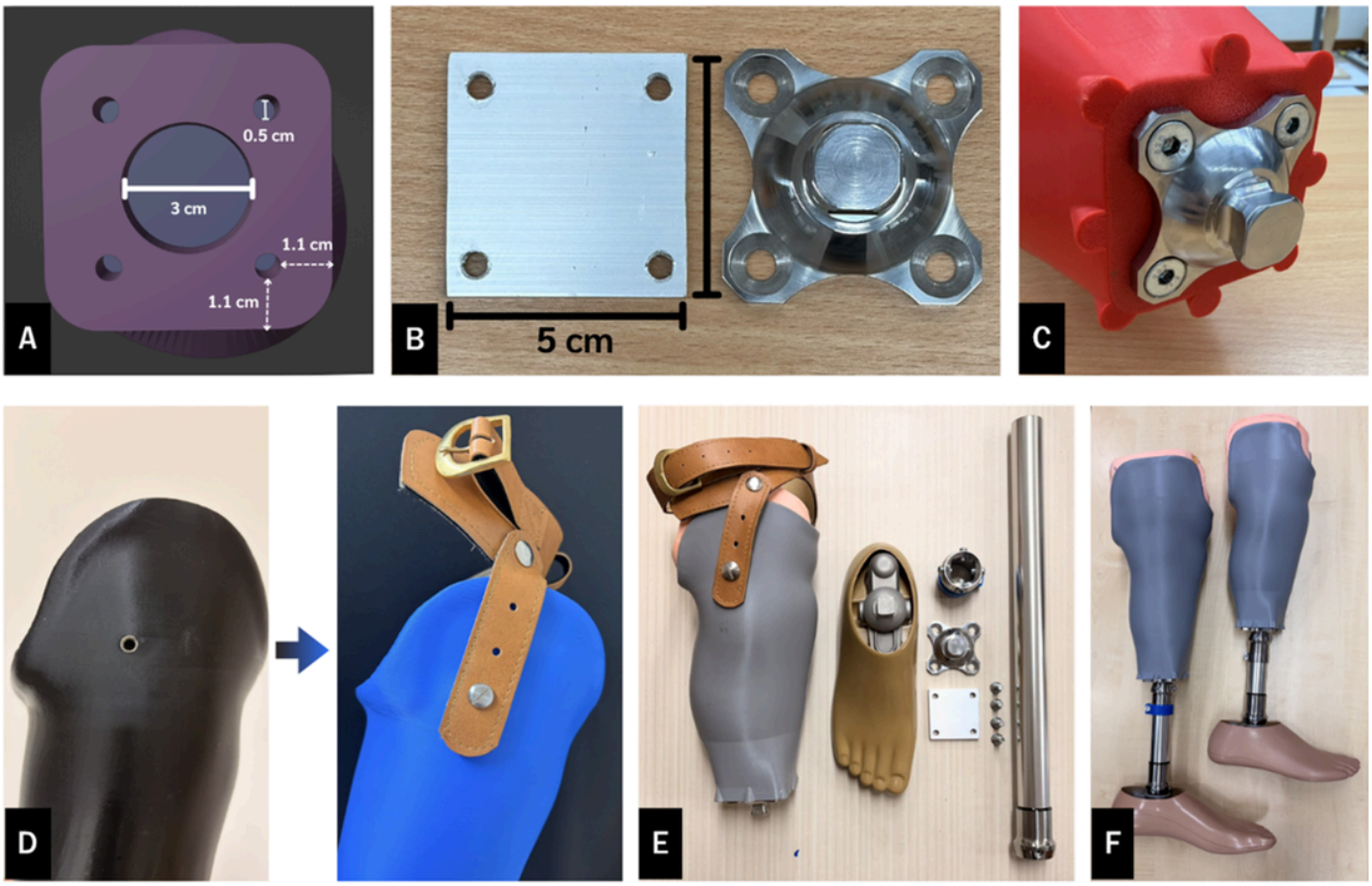


Figure 5

(A) Adapter holes in CAD software, (B) Metal plate with drilled holes, (C) Assembly of distal end, (D) Cuff strap suspension attachment, **(E)** Prosthetic components, and **(F)** the assembled 3D-printed prostheses



Figure 6

3D-printed transtibial prostheses during donning in coronal (left) and sagittal planes (right)

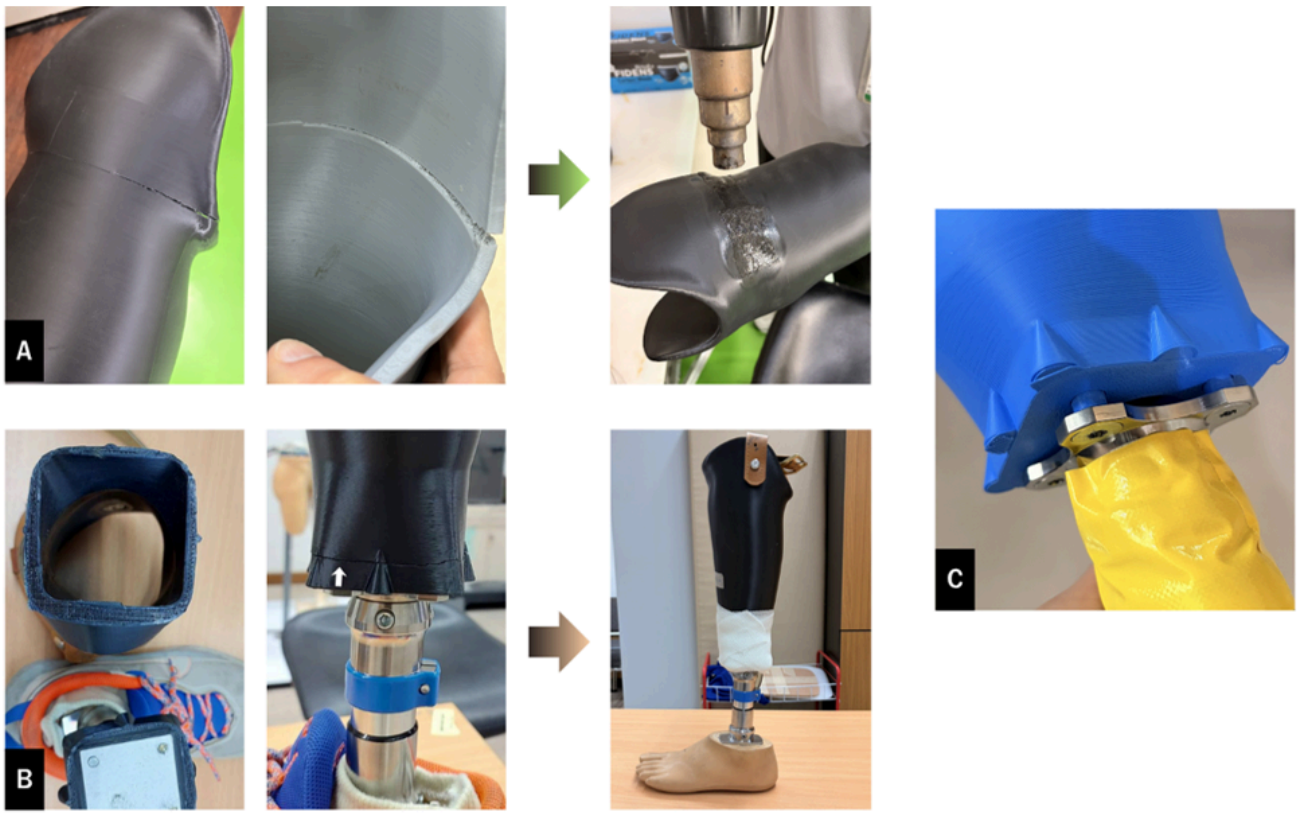


Figure 7

Problems found after usage: (A) Crack along the medial brim and temporary solution, (B) Breakage at the connection area and temporary solution, and (C) Breakage of the filament around two posterior screws of the distal end adapter